J|A|C|S
ARTICLES

Published on Web 08/02/2010

Asprich Peptides Are Occluded in Calcite and Permanently Disorder Biomineral Crystals

Rebecca A. Metzler,[†] Gareth A. Tribello,[‡] Michele Parrinello,[‡] and P. U. P. A. Gilbert*[,†,§]

Department of Physics, University of Wisconsin—Madison, 1150 University Avenue, Madison, Wisconsin 53706, Computational Science, Department of Chemistry and Applied Biosciences, ETH Zurich USI-Campus, Via Giuseppe Buffi 13, C-6900 Lugano, Switzerland

Received April 12, 2010; E-mail: pupa@physics.wisc.edu

Abstract: Macromolecules are a minority but important component of the minerals formed by living organisms, or biominerals. The role these macromolecules play at the early stages of biomineral formation, as well as their long-term and long-range effects on the mature biomineral, is poorly understood. A 42-amino acid peptide, asp2, was derived from the Asprich family of proteins. In this study we present X-ray absorption near-edge structure spectroscopy and X-ray photoelectron emission microscopy data from the asp2 peptide, the calcite ($CaCO_3$) crystals, and the peptide + crystal composites. The results clearly show that asp2 is occluded in fully formed biomineral crystals and slightly but permanently disorders the crystal structure at short- and long-range distances.

Introduction

Biominerals are composites of organic molecules and minerals that serve a variety of functions in different organisms. Despite the small percentage of organics (0.1−5 wt %[1,2]), biomineral composites have vastly different materials properties compared to their geologic counterparts. In the past 2 years, several unexpected observations have been reported: the existence of prenucleation clusters in calcium and carbonate solutions,[3] organic−mineral templation at the nanoscale,[4] multiple amorphous precursor phases,[5] the effect of organic molecules on Mg/Ca concentration ratios,[6] and lamellar self-assembly of a single peptide and aragonite resembling natural nacre.[7] All this work addressed the possible steps that occur during the dynamic process of biomineral formation; however, the role played by organic molecules in the process remains elusive.

The molecular-scale interaction between the organic and the mineral components throughout biomineral formation is key to understanding the formation mechanism of biomineral composites. Due to the complexity of biomineralizing organisms, it is extremely difficult or impossible to identify individual participants and events during biomineralization. A tractable alternative is to use a limited number of key components under controlled conditions and to examine the formation of model biominerals in the laboratory. While model biomineral systems convey limited information due to their inherent simplicity, such systems have been shown to provide much-needed insight into the roles organic molecules play in stabilizing amorphous calcium carbonate (ACC),[6,8,9] in polymorph selection,[10−12] in crystal growth inhibition,[13−15] and more.

Here we examine the role of the organic−mineral interaction during and after the biomineral formation process in a model biomineral system. Many recent studies have highlighted the importance of acidic amino acids in enabling the organic−mineral interaction.[16,17] One family of seven proteins, Asprich a−g (Figure S1, Supporting Information), extracted from the prismatic layer of *Atrina rigida* shell, was found to have a highly acidic, conserved, 42-amino acid domain at its C-terminus,[18]

[†] University of Wisconsin−Madison.
[‡] ETHZ Zurich USI-Campus.
[§] Previously publishing as Gelsomina De Stasio.

(1) Hare, P. E.; Abelson, P. H. *Carnegie Inst. Washington Yearb.* **1965**, *64*, 223–234.
(2) Wilt, F. *J. Struct. Biol.* **1999**, *126*, 216–226.
(3) Gebauer, D.; Volkel, A.; Cölfen, H. *Science* **2008**, *322*, 1819–1822.
(4) Pouget, E. M.; Bomans, P. H. H.; Goos, J. A. C. M.; Frederik, P. M.; de With, G.; Sommerdijk, N. A. J. M. *Science* **2009**, *323*, 1455–1458.
(5) Politi, Y.; Metzler, R. A.; Abrecht, M.; Gilbert, B.; Wilt, F. H.; Sagi, I.; Addadi, L.; Weiner, S.; Gilbert, P. U. P. A. *Proc. Natl. Acad. Sci. U.S.A.* **2008**, *105*, 17362–17366.
(6) Wang, D.; Wallace, A. F.; De Yoreo, J. J.; Dove, P. M. *Proc. Natl. Acad. Sci. U.S.A.* **2009**, *106*, 21511–21516.
(7) Metzler, R. A.; Evans, J. S.; Killian, C. E.; Zhou, D.; Churchill, T.; Appathurai, N. P.; Coppersmith, S. N.; Gilbert, P. U. P. A. *J. Am. Chem. Soc.* **2010**, *132*, 6329–6334.
(8) Aizenberg, J.; Lambert, G.; Addadi, L.; Weiner, S. *Adv. Mater.* **1996**, *8*, 222–226.
(9) Aizenberg, J.; Lambert, G.; Weiner, S.; Addadi, L. *J. Am. Chem. Soc.* **2002**, *124*, 32–39.
(10) Feng, Q. L.; Pu, G.; Pei, Y.; Cui, F. Z.; Li, H. D.; Kim, T. N. *J. Cryst. Growth* **2000**, *216*, 459–465.
(11) Samata, T.; Hayashi, N.; Kono, M.; Hasegawa, K.; Horita, C.; Akera, S. *FEBS Lett.* **1999**, 462.
(12) Suzuki, M.; Saruwatari, K.; Kogure, T.; Yamamoto, Y.; Nishimura, T.; Kato, T.; Nagasawa, H. *Science* **2009**, *325*, 1353–1390.
(13) Elhadj, S.; De Yoreo, J. J.; Dove, P. M. *Proc. Natl. Acad. Sci. U.S.A.* **2006**, *103*, 19237–19242.
(14) Mann, K.; Siedler, F.; Treccani, L.; Heinemann, F.; Fritz, M. *Biophys. J.* **2007**, *93*, 1246–1254.
(15) Politi, Y.; Mahamid, J.; Goldberg, H.; Weiner, S.; Addadi, L. *CrystEngComm* **2007**, *9*, 1171–1177.
(16) Delak, K.; Collino, S.; Evans, J. S. *Langmuir* **2007**, *23*, 11951–11955.
(17) Metzler, R. A.; Kim, I. W.; Delak, K.; Evans, J. S.; Zhou, D.; Beniash, E.; Wilt, F.; Abrecht, M.; Chiou, J. W.; Guo, J.; Coppersmith, S. N.; Gilbert, P. U. P. A. *Langmuir* **2008**, *24*, 2680–2687.
(18) Gotliv, B. A.; Kessler, N.; Sumerel, J. L.; Morse, D. E.; Tuross, N.; Addadi, L.; Weiner, S. *Chem. Bio. Chem.* **2005**, *6*, 305–314.

DEADEADADEADADEADADNDAADETDAADVGTEAEDVADDE

Figure 1. Sequence of the Asprich fragment 2 (asp2) peptide.[48] This sequence is the C-terminus domain in all Asprich proteins a−g (Figure S1, Supporting Information).[18] Asp2 is highly acidic, containing 23 acidic amino acids, Asp (D) and Glu (E), highlighted in red, out of the total 42 amino acids.

termed asp2, as shown in Figure 1. Our model biomineral system consists of the initial growth of a seed calcite crystal and subsequent overgrowth of calcite in the presence of asp2. This overgrowth strategy enables the simultaneous analysis of the inner control crystal and the model composite biomineral on the outer zone of the same crystal, thus providing a unique opportunity to quantitatively compare the inner and outer zones, and thereby establish the effect asp2 has on calcite crystal growth.

To examine the molecular-scale interactions between the organic and mineral components, we used X-ray absorption near-edge structure (XANES) spectroscopy and X-ray photoelectron emission microscopy (X-PEEM), which provide spatial resolution and information about the electronic and molecular structure in the immediate vicinity of the atoms probed spectroscopically. The use of XANES and X-PEEM on model overgrown biominerals directly addresses several questions: whether and how the organic molecule is incorporated in the forming crystal, how the mineral *and* the organic molecule affect one other, and whether and how the interactions at the organic−mineral interface change at the onset and during the course of biomineral formation, that is, how they evolve in the outer zone as a function of distance from the inner zone.

Results

The crystal inner zone was grown from a 10 mM $CaCl_2$ solution and ammonium carbonate diffusion. The outer zone is the result of overgrowth from the same solution, to which asp2 was added to a final concentration of 100 μM. The calcite + asp2 growth resulted again from ammonium carbonate diffusion. The final two-zone crystals were embedded in epoxy and polished until the crystal section could be observed with visible light microscopy (VLM), as shown in Figures S2 and S8 (Supporting Information). This preparation made both the inner and outer zones of each crystal accessible to X-PEEM/XANES spectroscopy. Comparison of carbon, oxygen, and calcium spectra of the inner and outer zones of the crystals shows clear and dramatic spectral differences, due to the interaction of the organic and the mineral components. We examined a total of 25 crystals from two different crystal growths with X-PEEM and 75 crystals with VLM; the spectra, sizes, and shapes were consistent with those presented in Figures 2 and S2.

In the carbon K-edge spectrum (Figure 2A), the asp2 peptide exhibits peaks well-known to be associated with organics: a strong π^* peak at 288.2 eV associated with the C═O amide and carboxylate bonds and a weak σ^* peak at 287.2 eV associated with the C−H bond.[19] The carbon spectrum from the inner control crystal has peaks well-known to be associated with calcium carbonates, namely, a π^* peak at 290.3 eV and a series of three σ^* post-edge peaks at 295.5, 298.4, and 301.5

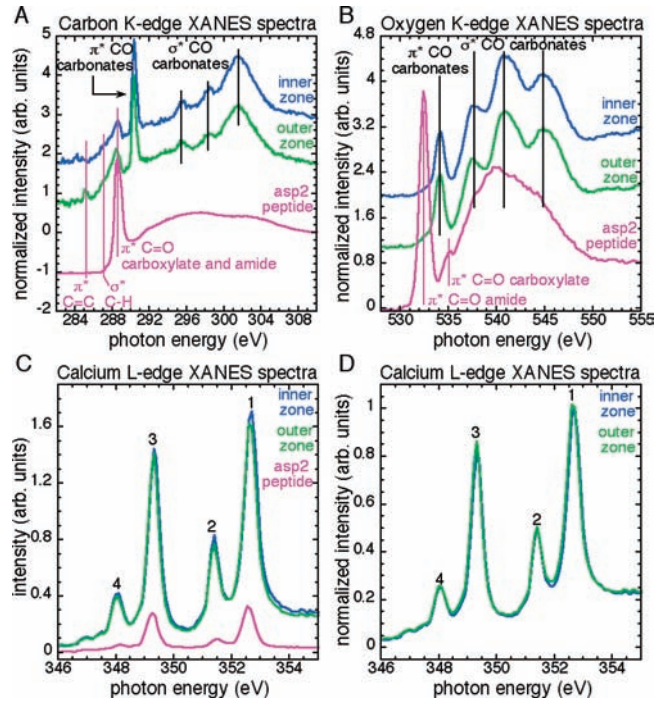

Figure 2. Spectra extracted from the asp2 peptide (magenta), the calcite crystal (inner zone, blue), and the overgrown calcite + asp2 composite crystal (outer zone, green). The inner zone represents a control calcite crystal, grown in solution with no additives, while the outer zone is the model biomineral composite of calcite and occluded asp2 peptide. The regions from which the spectra were extracted are shown in Figure S7 (Supporting Information). (A) Comparison of outer-zone carbon K-edge XANES spectrum to the inner-zone and asp2 peptide spectra. Spectra extracted from regions throughout the outer zone (not shown) exhibit no spectroscopic differences. Organic peaks are shown by vertical lines in magenta; carbonate peaks are shown by vertical lines in black. Quantitative peak-fitting results can be found in Figure S3 and Table S1 (Supporting Information). (B) Oxygen K-edge XANES spectrum extracted from the outer zone of the crystal compared to the crystal inner zone and peptide spectra. Once again, organic peaks are highlighted by magenta vertical lines and carbonate peaks by black vertical lines. Quantitative spectral differences are highlighted by peak fitting, shown in Figure S4 and Table S2 (Supporting Information). From the intensity of peak 1 in Figure S4B, we can estimate the amount of asp2 in the outer zone. (C) Un-normalized calcium L-edge XANES spectra from the inner and outer zones show a decrease in Ca concentration in the composite outer zone. Unexpectedly, the peptide also exhibits a low-intensity calcium signal, most likely from solution contamination, which demonstrates the peptide's strong affinity for calcium binding; this spectrum is dramatically different from the other two, with noticeable peak 2 and peak 4 lower intensity and energy splitting from peaks 1 and 3. The three spectra were divided by the background but not normalized in intensity. They were overlapped to the same baseline intensity here for a visual comparison of their different intensities. (D) Inner- and outer-zone calcium L-edge XANES spectra, normalized to have intensity 1 at peak 1. This comparison highlights the small differences in all peak widths, which are broader in the outer zone. Correspondingly, the dips between the L_2 peaks (peaks 1 and 2) and the L_3 peaks (peaks 3 and 4) are less deep. Because of the larger separation in energy of peaks 2 and 3, the depth of the dip between them is unchanged. Quantitative parameters from peak fitting can be found in Figure S5 and Table S3 (Supporting Information).

eV that are all associated with the CO carbonate bond.[17,20] The control crystal spectrum also exhibits peaks at 288 and 287 eV, which are consistently observed in calcite and aragonite[17,20] but have not yet been assigned. Notice that the outer-zone carbon spectrum reveals a distinctly different line shape compared to

(19) Kaznacheyev, K.; Osanna, A.; Jacobsen, C.; Plashkevych, O.; Vahtras, O.; Agren, H.; Carravetta, V.; Hitchcock, A. P. *J. Phys. Chem. A* **2002**, *106*, 3153–3168.

(20) Zhou, D.; Metzler, R. A.; Tyliszczak, T.; Guo, J.; Abrecht, M.; Coppersmith, S. N.; Gilbert, P. U. P. A. *J. Phys. Chem. B* **2008**, *112*, 13128–13135.

what would be expected from a simple linear combination of control calcite crystal (inner zone) and asp2 (Figure S6, Supporting Information). Specifically, the outer-zone spectrum shows a decrease in the intensity of the carbonate peaks compared to the control crystal, an increase in the C−H peak compared to both the asp2 peptide and control crystal, and the appearance of a π^* peak at 285 eV that is known to be associated with C═C bonds in amino acids.[19]

Similarly, the oxygen K-edge spectrum of the outer zone (Figure 2B) is different from the asp2 peptide spectrum, the inner-zone spectrum, or a linear combination of the two (Figure S6). The asp2 peptide spectrum contains two π^* peaks, located at 532.5 and 534.6 eV, which are associated with the oxygen atoms in the amide and the carboxylate bonds, respectively,[21] and a broad post-edge hump. The spectrum of the inner-zone control crystal consists of a π^* peak at 534 eV, a post-edge hump, and three prominent σ^* peaks at 540.6, 542.2, and 545 eV, all assigned to the oxygen in the CO carbonate bond. As observed for carbon, in the outer zone the carbonate oxygen peaks decrease in magnitude compared to the inner zone. In addition, upon peptide−mineral binding, a small π^* peak associated with the amide bond in the asp2 peptide appears in the spectrum of the outer zone. Consistent with its much smaller amplitude in asp2, the π^* carboxylate peak does not appear in the outer zone. The amplitude of the small amide peak (peak 1 in Figure S4 and Table S2, Supporting Information) is 3% of that in the pure asp2. This indicates that 3% of the oxygen atoms present in a probed voxel (3 nm deep, 200 nm × 200 nm wide) are in an asp2 peptide. With simple algebra, this result is converted to the statement that there are 2 mmol of asp2 per mole of calcite in the composite outer zone. This corresponds to 9.2 wt % asp2 in calcite.

The spectral changes in the calcium spectrum are small in magnitude but are nonetheless significant. In Figure 2C, the unnormalized calcium L-edge XANES spectra of the asp2 peptide, inner zone, and outer zone are reported. In these spectra the peak intensities are directly proportional to the Ca concentration in each sample. While the asp2 peptide should, in theory, have no calcium, the spectrum shows that there is a calcium signal. The presence of calcium in the asp2 peptide indicates calcium contamination of one of the solutions during peptide synthesis. However, the amount of calcium in the asp2 peptide is significantly smaller than that in the inner-zone and outer-zone crystals. As shown in Figure 2C, comparison of the inner- and outer-zone calcium spectra shows that both inner and outer zones are calcite[5,7,22,23] and the outer zone has a lower concentration of calcium than the inner zone. In Figure 2D we present the normalized spectra from the inner and outer zones of the crystal. There is slight broadening of all peaks in the outer zone, which is due to greater disorder in the CaO bonds.[24]

Component analysis was done for Ca spectra, and the resulting component maps are shown in Figure 3. In these maps two spectral components were selected: the inner- and outer-zone spectra presented in Figure 2D. Component maps were produced using the Gilbert group (GG) macros, a set of XANES spectromicroscopy analysis code written by our group for IGOR Pro, available free to interested researchers.[25] Stacks of X-PEEM images were collected while scanning the photon energy across the Ca L-edge. Thus, each pixel contains the full XANES spectrum. A linear combination of the two component spectra is calculated, enabling energy shifts, to best-fit each pixel spectrum, and then the proportion of each component is displayed in a different color (see Figure 3 labels) and combined according to the additive color mixing rules.[26] The component map of Figure 3 shows that the outer zone of the crystal is spatially distinct from the inner zone of the crystal, therefore confirming that the spectrum from the outer zone is spectroscopically distinct from the inner-zone spectrum. Specifically, notice that the outer zone of the crystal forms a thick border around the inner zone, indicating that each pixel of the crystal grown in the presence of asp2 exhibits a modified spectrum representative of an organic−mineral interaction and that the results presented in Figure 2 are extremely consistent and statistically representative of the entire model biomineral. The

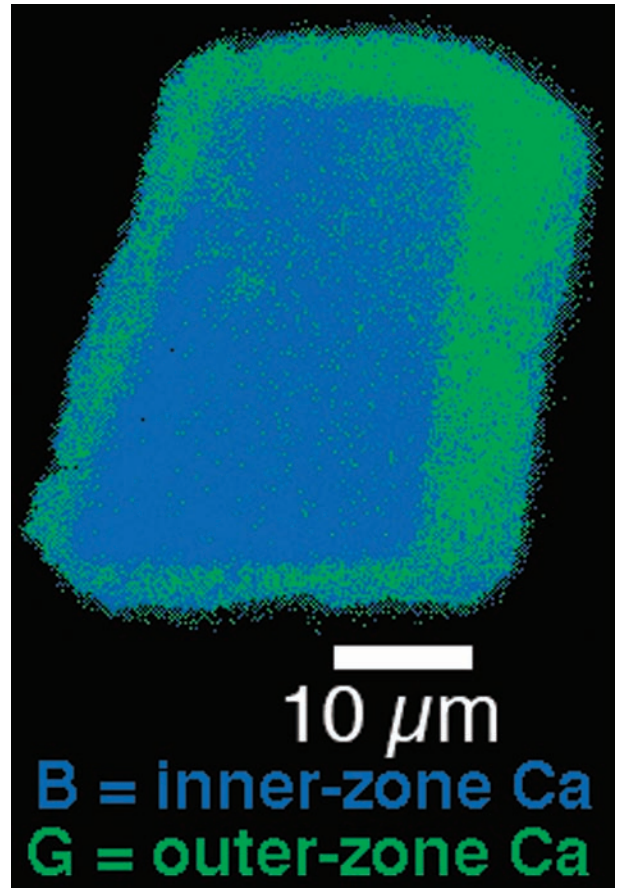

Figure 3. Component map of the inner and outer zones. This map was obtained by best-fitting the spectrum from each pixel with two spectral components: the Ca spectrum from the inner (blue) and the outer (green) zones, respectively. The component map shows a sharp separation between the inner and outer zones and no mixing of the two (cyan). Further evidence of spectroscopic differences in the inner and outer zones is presented in Figure S2 (Supporting Information).

(21) Stewart-Ornstein, J.; Hitchcock, A. P.; Hernandez Cruz, D.; Henklein, P.; Overhage, J.; Hilpert, K.; Hale, J. K.; Hancock, R. E. *J. Phys. Chem. B* **2007**, *111*, 7691–7699.
(22) Benzerara, K.; Yoon, T. H.; Tyliszczak, T.; Constantz, B.; Spormann, A. M.; Brown, G. E. *Geobiology* **2004**, *2*, 249–259.
(23) Killian, C. E.; Metzler, R. A.; Gong, Y. U. T.; Olson, I. C.; Aizenberg, J.; Politi, Y.; Wilt, F. H.; Scholl, A.; Young, A.; Doran, A.; Kunz, M.; Tamura, N.; Coppersmith, S. N.; Gilbert, P. U. P. A. *J. Am. Chem. Soc.* **2009**, *131*, 18404–18409.
(24) de Groot, F. M. F.; Fuggle, J. C.; Thole, B. T.; Sawatzky, G. A. *Phys. Rev. B* **1990**, *41*, 928–937.
(25) The GG macro can be downloaded free of charge from http://home.physics.wisc.edu/gilbert/, click on "Software".
(26) Gilbert, P. U. P. A.; Haeberli, W. *Physics in the Arts*; Elsevier-Academic Press: Burlington, MA, 2008.

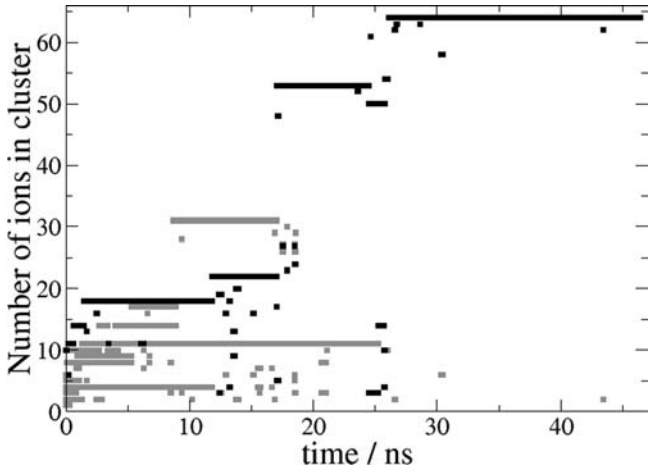

Figure 4. Cluster sizes that are present in solution as a function of simulation time. Black lines are those clusters that have one atom within 5 Å of one of the atoms in the peptide, and gray lines are those that are farther away.

Ca components map shows an abrupt and sharp separation of the inner and the outer zones. The absence of cyan pixels in Figure 3 indicates that no mixture of the green and blue components is present at the 200-nm pixel resolution of this map.

To further explore the interaction of the asp2 peptide with calcium carbonate during the early stages of crystal formation, we performed molecular dynamics simulations at an elevated calcium carbonate concentration and at a temperature of 300 K.[27] Simulating the entire 42-residue peptide would be very computationally expensive; thus, we modeled a five-residue portion of the sequence, DEADA, which is repeated three times in asp2. This portion was terminated using an acetyl group at its N-terminus and an N-methyl group at its C-terminus. This DEADA peptide was placed in a box of 6985 water molecules along with 32 randomly distributed calcium ions and 32 randomly distributed carbonate ions — a concentration of 0.251 mol/L. Figure 4 shows that amorphous calcium carbonate clusters form during the simulation, as was seen in the absence of peptides in ref 27, and that these $CaCO_3$ amorphous clusters attach themselves to the peptide. This suggests that the peptide binds strongly to prenucleation clusters.

Discussion

The data of Figures 2 and 3 provide clear evidence that the asp2 peptide is *occluded* in the fully formed mineral and quantitative information on the organic−mineral interaction within the biomineral. Specifically, the presence of a small C═O amide peak in the O spectrum of the outer zone (Figure S4B, Supporting Information) can only be assigned to a small concentration of peptide in this overgrown model biomineral. Oxygen spectra from pure calcite do not show this peak. Similarly, the concentration of Ca in the outer zone is significantly lower than in the inner zone, yet the calcium spectrum is clearly similar to that of calcite.[5,7,22,23] The only possible explanation for a decreased "calcite calcium" density in a calcite crystal is the presence of another non-calcite component, and this can only be asp2.

The occlusion of organic molecules has been previously observed in natural biominerals, such as the LSM34 protein occluded in calcitic sea urchin spicules,[28] the unidentified proteins in mollusk shell nacre and prismatic crystals,[29−31] or the protein occluded in a model sea urchin skeleton biomineral system.[32] However, the work presented here is the first direct evidence of occlusion inside a model, polished, mollusk shell biomineral. Examination of the polished crystal cross-section provides the unique capability of examining the bulk of the crystal, rather than the surface, as is done in scanning electron microscopy (SEM) or fluorescence experiments.

Furthermore, there is unequivocal evidence for peptide−mineral binding in C spectra of the outer zone. It is important to note that chemical bonds are formed between the asp2 peptide and the mineral crystal; the peptide is not simply trapped within the mineral and therefore only physically present — it is chemically interacting. The C−H bond peak in the outer-zone carbon spectrum increases in magnitude in comparison to that in the inner-zone carbon spectrum. The majority of C−H bonds are in amino acid side chains, and one C−H per amino acid is in the main chain of proteins and peptides, at the C_α location. In solution the asp2 peptide is unstructured and its conformation is labile;[33] thus, both the side chains and the main chain of the asp2 peptide are disordered. In XANES spectroscopy, a higher and narrower peak corresponds to a more ordered system, in which all similar bonds are aligned. It is possible, as suggested by Metzler et al.,[17] that the C−H peak enhancement results from an increase in order of the peptide side chains. It is also possible, and perhaps more likely, that the C_α−H bonds on the main chain become more co-oriented after mineral binding, as was shown for statherin.[34,35] Although we do not know which C−H bonds are ordering, we do know with certainty that, after peptide−mineral binding, the peptide restructures and acquires a more ordered secondary structure. The carbon spectra are consistent throughout the outer zone, including the outer surface of the crystal, indicating that the structures of the surface-bound peptide and occluded-bound peptide must be similar. A recent study by He et al. found that structural ordering occurs when the dental matrix protein 1 (DMP1), which is present in the mineralized matrix of bone and dentin, binds calcium, changing from a random coil to a β-sheet, resulting in greater alignment of the C_α−H bonds on the main chain.[36]

In addition, the decreased intensity of the carbonate CO bonds' peaks in C and O spectra can only be interpreted as a disruption of CO carbonate bonds' co-orientation in the crystal when peptides are occluded. Note that this intensity decrease is on the order of 10−30% for the various peaks (see Table S2, Supporting Information) and cannot correspond to an overall decrease in calcite density, which is on the order of 9%. The decrease in CO peaks intensity, therefore, must originate from

(27) Tribello, G. A.; Bruneval, F.; Liew, C. C.; Parrinello, M. *J. Phys. Chem. B* **2009**, *113*, 11680–11687.
(28) Killian, C. E.; Wilt, F. H. *J. Biol. Chem.* **1996**, *271*, 9150–9159.
(29) Pokroy, B.; Fitch, A. N.; Lee, P. L.; Quintana, J. P.; Caspi, E. N.; Zolotoyabko, E. *J. Struct. Biol.* **2006**, *153*, 145–150.
(30) Pokroy, B.; Fitch, A. N.; Marin, F.; Kapon, M.; Adir, N.; Zolotoyabko, E. *J. Struct. Biol.* **2006**, *155*, 96–103.
(31) Pokroy, B.; Quintana, J. P.; Caspi, E. N.; Berner, A.; Zolotoyabko, E. *Nat. Mater.* **2004**, *3*, 900–902.
(32) Berman, A.; Addadi, L.; Weiner, S. *Nature* **1988**, *331*, 546–548.
(33) Delak, K.; Collino, S.; Evans, J. S. *Biochemistry* **2009**, *38*, 3669–3677.
(34) Shaw, W. J.; Long, J. R.; Dindot, J. L.; Campbell, A. A.; Stayton, P. S.; Drobny, G. P. *J. Am. Chem. Soc.* **2000**, *122*, 1709–1716.
(35) Stayton, P. S.; Drobny, G. P.; Shaw, W. J.; Long, J. R.; Gilbert, M. *Crit. Rev. Oral. Biol. Med.* **2010**, *14*, 370–376.
(36) He, G.; Gajjerman, S.; Schultz, D.; Cookson, D.; Qin, C.; Butler, W. T.; Hao, J.; George, A. *Biochemistry* **2005**, *44*, 16140–16148.

a 10−30% lower number of *co-oriented* CO bonds, and not only from a 3% lower number of overall CO bonds, however oriented.

An important conclusion is that the modifications to the crystal structure resulting from the interaction with the peptide occur not only at the beginning of the peptide−crystal interaction, that is, at the onset of biomineralization, but also continue later on, in the mature biomineral. The changes in the crystal electronic structure are *permanent*.

In Ca spectra, the observed decrease in the depth of the dips between all peaks further supports the conclusion that the interaction with the peptide disrupts the crystal structure and ordering. The energy regions of peaks 2 and 4 in calcium spectroscopy are affected by the crystal field, which originates from the symmetry of atoms surrounding the calcium atom:[24,37] a symmetry-altering peptide−mineral interaction would result in a change in energy position or intensity of peaks 2 and 4, which is not observed. We conclude, therefore, that the peptide−mineral interaction does not alter the calcite octahedral symmetry, and the Ca coordination remains 6 in biomineral calcite, synthetic or biogenic.[5]

The Ca spectra show slight peak broadening, which is consistent across all main Ca spectral features (see peak widths of peaks 1−4 in Table S3, Supporting Information). This broadening results in a less deep dip between nearby peaks 1 and 2, and peaks 3 and 4. Although this decrease in dip depth was not previously reported in biominerals at the Ca L-edge, in FeOOH minerals such lowering of dip depth in Fe L-edge spectra was directly associated with a decrease in crystalline long-range order, as detected by X-ray diffraction.[38] Since XANES spectroscopy is most sensitive to the first and second atomic shells surrounding the atom under analysis,[39] and *all* peak widths are affected, not just the crystal field peaks at the Ca L-edge, we conclude that the peak broadening observed here is due to disruption of *short-range* order. In this article short-range is defined as within 15 Å of the probed atom, as previously determined by Farges et al.[40]

Long-range order disruption in natural biomineral systems resulting from the presence of organic molecules within the biomineral was previously reported in several high-resolution X-ray diffraction studies.[29−31] Here we provide a direct, simultaneous, and quantitative analysis of short-range order disruption on the *same* crystal; such short-range order disruption has previously only been observed in biogenic aragonite.[41]

We note that the crystalline order observed by XANES at the Ca L-edge in the synthetic calcite biomineral here, or in biogenic calcites previously studied,[5] is not as pronounced as in pure calcite. Evidently, proteins and peptides may affect the crystal electronic structure at the short-range, as observed here, at the medium-range, as detected by the crystal field peaks,[5] and at the long-range, as detected by diffraction in diverse biominerals.

The peptide is observed here to have a short-range effect. This effect is not limited to the time and location of peptide−mineral interaction during biomineral formation but persists everywhere across the biomineral and is *permanent* in time once the mineral is formed. This observation raises an important question: How does the short-range disorder detected here propagate to long-range distances?

The small concentration of peptide occluded in the biomineral (9.2 wt %), which is slightly higher than other natural biominerals, suggests a long-range effect. The solution to the puzzle lies in the asp2 peptide interaction with ions in solution and prenucleation clusters of $CaCO_3$. The Cölfen group showed that small clusters of calcium carbonates form in solution.[3] Molecular dynamics simulations by the Parrinello group showed that free calcium and carbonate ions in solution quickly combine to form calcium carbonate nanoclusters, and that the growth of these amorphous nanoparticles is essentially diffusion-controlled.[27,42] In addition, they showed that when these clusters are small (three or four ions) they have a chain-like structure, and that with further growth they become globular. In a separate study, they also showed that these ions bind strongly to carboxylate groups.[43] The simulations of Figure 4 suggest that the asp2 peptide binds strongly to prenucleation clusters. The Sommerdijk group showed experimentally that such small clusters in the proximity of templating organic molecules aggregate to form clusters of ACC up to a critical size and subsequently crystallize.[4]

All these recent results, combined with the present observation that asp2 is occluded into the crystal and significantly and permanently affects the crystal electronic structure at the short-range, concur and suggest the model for the early stages of biomineral formation presented in Figure 5. In this model the asp2 peptide binds to the ions and prenucleation clusters in the $CaCO_3$ growth solution rather than binding directly to the surface of the seed crystal. As shown by the imperfect crystalline order in Figure 5, strain, distortions, and disorder may persist on a scale much greater than a few unit cells, as the crystal growth is epitaxial (step 8) on a strained and distorted substrate, even far away from the peptide. The cartoon in Figure 5 explains how a small concentration of peptide can affect the structure of the entire crystal, as observed in many biominerals.[29−31] Future spectroscopy and diffraction experiments, and more-detailed simulations, based on atomistic molecular dynamics of the early stages of biomineral formation will confirm or refute this cartoon model.

In conclusion, we present spectromicroscopy data clearly showing that the asp2 peptide is occluded in the fully formed calcite + asp2 biomineral composite. Asp2 permanently disrupts short-range order in the composite biomineral. Further epitaxial growth preserves the disordered structure induced by just a few organic molecules.

Materials and Methods

Extensive experimental details are provided in the Supporting Information. We briefly describe here the sample growth, X-PEEM experiment, and data analysis procedures.

***In Vitro* Mineralization.** *In vitro* calcium carbonate growth was done in 10 mM $CaCl_2$ solutions, exposed to ammonium carbonate $[(NH_4)_2CO_3]$ vapors. The control seed crystal was grown for 24 h in the absence of asp2. At the conclusion of growth, the crystals were removed from the growth solution, washed with calcium

(37) Naftel, S. J.; Sham, T. K.; Yiu, Y. M.; Yates, B. W. *J. Synch. Radiat.* **2001**, *8*, 255–257.
(38) Chan, C. S.; De Stasio, G.; Welch, S. A.; Girasole, M.; Frazer, B. H.; Nesterova, M. V.; Fakra, S.; Banfield, J. F. *Science* **2004**, *303*, 1656–1658.
(39) Stohr, J. *NEXAFS spectroscopy*; Springer-Verlag: Berlin, Germany, 1992.
(40) Farges, F.; Brown, G. E.; Rehr, J. J. *Phys. Rev. B* **1997**, *56*, 1809–1819.
(41) Pokroy, B.; Fieramosca, J. S.; Von Dreele, R. B.; Fitch, A. N.; Caspi, E. N.; Zolotoyabko, E. *Chem. Mater.* **2007**, *19*, 3244–3251.
(42) Bruneval, F.; Donadio, D.; Parrinello, M. *J. Phys. Chem. B* **2007**, *111*, 12219–12227.
(43) Bulo, R. E.; Donadio, D.; Laio, A.; Molnar, F.; Rieger, J.; Parrinello, M. *Macromolecules* **2007**, *40*, 3437–3442.

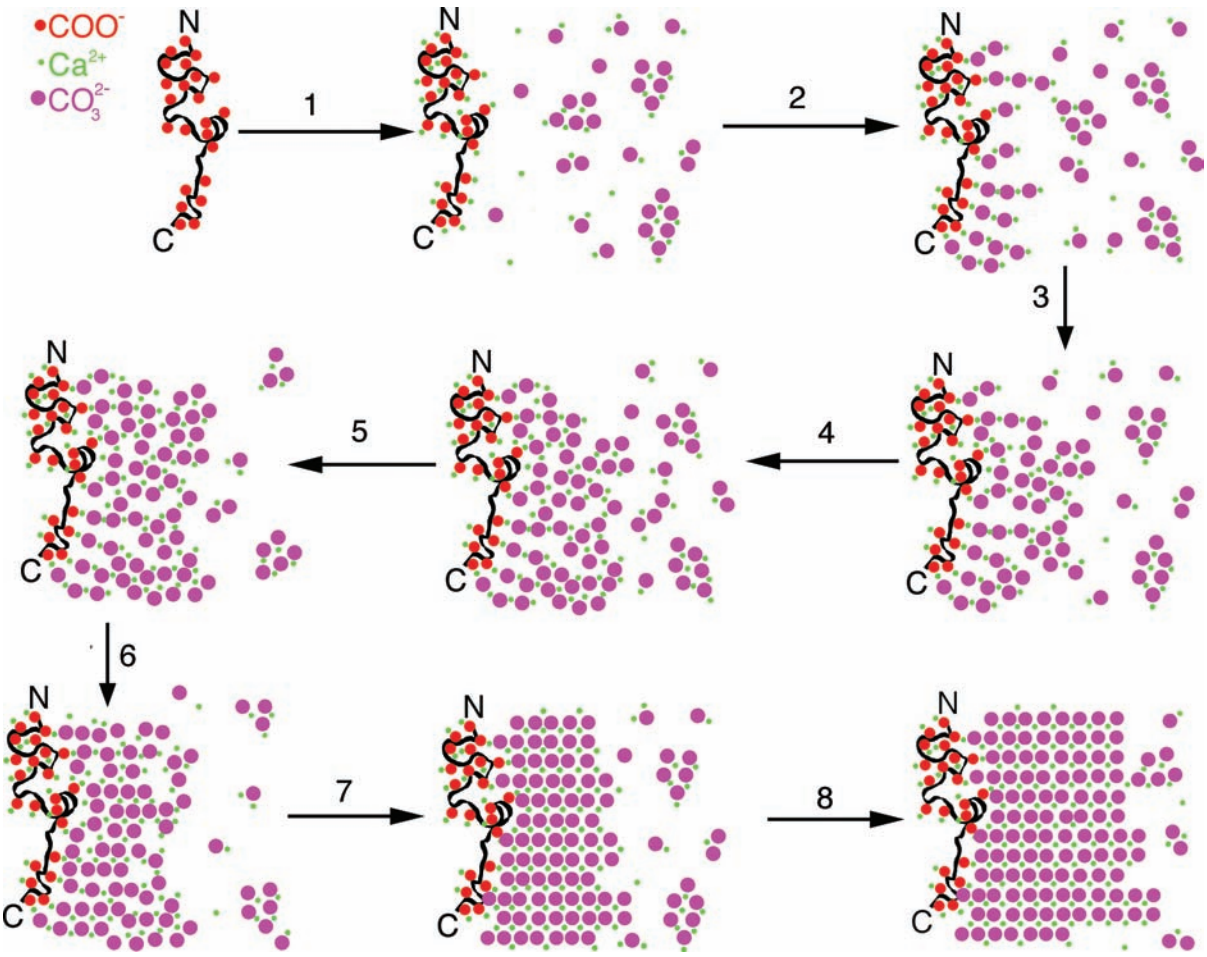

Figure 5. Schematic diagram of the early stages of biomineralization. Asp2 continuously changes conformation in solution, and it has 23 negatively charged residues, exposing their COO^- groups to solution (red). Step 1: COO^- forms ionic bonds with Ca^{2+} ions in solution, while other small clusters of ions appear and disappear in solution, independent of the peptide, and away from it. Step 2: Peptide-bound Ca^+ ions attract more ions and clusters of ions from the solution. These are short peptide-stabilized $CaCO_3$ chains. Step 3: More ions and clusters from solution join the aggregate and form globular structures. Further aggregation of $CaCO_3$ molecules and prenucleation clusters (steps 4 and 5) eventually reach a critical size (step 6) and start ordering into an intermediate disordered aggregate, which gradually excludes water. Step 7: The aggregate gradually becomes more ordered as more water is excluded. Step 8: The aggregate is now in its final crystalline structure and continues to grow at the expense of more ions and clusters from solution. The crystalline order observed is not perfect, as it would be in the absence of the peptide.

carbonate-saturated methanol, and air-dried. Half of the crystals were placed in a growth solution containing 10 mM $CaCl_2$ and 100 μM asp2, while the remaining crystals were placed in the control 10 mM $CaCl_2$ growth solution, and allowed to grow for 24 h. A total of 75 crystals were examined with visible light microscopy (VLM), and all revealed an overgrowth layer, which was not observed in the controls. The dimensions of the overgrown asp2 + calcite and overgrown calcite (control) samples were consistently comparable. More crystal images are presented in Figures S2 and S8 (Supporting Information).

X-PEEM. Overgrowth crystals were embedded in epoxy, polished, and Pt-coated for X-PEEM analysis on the SPHINX microscope as described in ref 44. In an X-PEEM experiment, the sample is imaged while scanning the illuminating photon energy. Therefore, each pixel in the image contains the full XANES spectrum across the C K-edge, O K-edge, and Ca L-edge. XANES spectroscopy is sensitive to the electronic structure surrounding the atom under analysis (C, O, or Ca in this work) and provides information on the presence and chemical state of elements in the sample, including relative concentration and crystal structure. X-PEEM spatial resolution can go down to 10 nm,[45] although for spectral analysis the pixel size is usually larger (20 nm or greater) to reduce experimental noise.[46,47] In the present work the pixel size was 200 nm.

X-PEEM Data Processing. All data processing was done in Igor Pro using GG macros.[25] Individual spectra were extracted from selected regions of interest (Figure S7, Supporting Information) and normalized to a pre-edge linear background for calcium or a simultaneously acquired background for carbon and oxygen. Background removal was done simultaneously for both the inner and outer zones of the crystal, with the same background spectrum removed from each spectrum, to ensure reliability and eliminate the possibility that the observed spectral variations might be caused by normalization. All carbon and oxygen spectra were intensity-

(44) De Stasio, G.; Frazer, B. H.; Gilbert, B.; Richter, K. L.; Valley, J. W. *Ultramicroscopy* **2003**, *98*, 57–62.
(45) Frazer, B. H.; Girasole, M.; Wiese, L. M.; Franz, T.; De Stasio, G. *Ultramicroscopy* **2004**, *99*, 87–94.
(46) Killian, C. E.; Metzler, R. A.; Gong, Y. T.; Olson, I. C.; Aizenberg, J.; Politi, Y.; Addadi, L.; Weiner, S.; Wilt, F. H.; Scholl, A.; Young, A.; Coppersmith, S. N.; Gilbert, P. U. P. A. *J. Am. Chem. Soc.* **2009**, *131*, 18404–18409.
(47) Politi, Y.; Metzler, R. A.; Abrecht, M.; Gilbert, B.; Wilt, F. H.; Sagi, I.; Addadi, L.; Weiner, S.; Gilbert, P. U. P. A. *Proc. Natl. Acad. Sci. U.S.A.* **2008**, *105*, 17362–17366.
(48) Delak, K.; Giocondi, J.; Orme, C.; Evans, J. S. *Cryst. Growth Des.* **2008**, *8*, 4481–4486.

normalized so the pre-edge was 0 and the post-edge was 1; intensity-normalized Ca spectra were also set to a 0 pre-edge and the 352.6 eV peak to 1. After normalization, peak fitting was done to quantify the spectral differences between the inner and outer zones, with Gaussian or Voigt curves used for the spectral peaks and arctangents for the ionization potentials.[39] The choice of Gaussian versus Voigt depends on the specific peak being fitted and its line shape. During peak fitting we start with Gaussian curves for all peaks; if the fit residue shows a large discrepancy of the fit to the left and right of a peak, we try choosing a Voigt line shape instead, which is a linear combination of a Gaussian and a Lorentzian, which has more intensity on its tails. The experimental line shape of a peak depends on the instrumental resolution and the intrinsic lifetime-related width of the peak. As described by Stohr,[39] XANES peaks could be fitted by either curve. For all peaks the best fit was found to be with Gaussians, while for the carbonate π^* peak at 290.3 eV the best fit is consistently found using a Voigt function, in which the mixing is one of the fit parameter set free. The peak fitting was done first for the inner zone and then for the outer zone using the inner-zone coefficients as the starting point and adding in the ionization potentials associated with the organics. The data presented in Figures 1 and 2 were consistent with X-PEEM data acquired from 24 other crystals taken from two different growths.

Acknowledgment. We thank John S. Evans for providing the asp2 peptides and Benjamin Gilbert for developing the GG macros. This work was supported by NSF award DMR&CHE-0613972, DOE Award DE-FG02-07ER15899, and UW-Hamel Awards to P.U.P.A.G. The experiments were performed at the UW-SRC, supported by NSF award DMR-0537588.

Supporting Information Available: Detailed methods, eight figures, and three tables containing peak-fitting coefficients. This material is available free of charge via the Internet at http://pubs.acs.org.

JA103089R